AIP | Journal of Applied Physics

# Micro-Raman thermometry in the presence of complex stresses in GaN devices

T. Beechem, A. Christensen, S. Graham, and D. Green

Citation: J. Appl. Phys. **103**, 124501 (2008); doi: 10.1063/1.2940131
View online: http://dx.doi.org/10.1063/1.2940131
View Table of Contents: http://jap.aip.org/resource/1/JAPIAU/v103/i12
Published by the American Institute of Physics.

# Micro-Raman thermometry in the presence of complex stresses in GaN devices

T. Beechem,[1] A. Christensen,[1] S. Graham,[1,a)] and D. Green[2]
[1]*G.W. Woodruff School of Mechanical Engineering, Georgia Institute of Technology, Atlanta, Georgia 30332, USA*
[2]*RFMDR Infrastructure Product Group, Charlotte, North Carolina 28269, USA*

(Received 18 January 2008; accepted 13 April 2008; published online 16 June 2008)

Raman thermometry is often utilized to measure temperature in gallium nitride (GaN) electronics. However, the accuracy of the technique is subject to errors arising from stresses which develop during device operation as a result of both thermoelastic and inverse piezoelectric effects. To assess the implications of these stresses on Raman thermometry, we investigate the use of the Stokes peak position, linewidth, and Stokes to anti-Stokes intensity ratio to estimate the temperature of GaN devices during operation. Our results indicate that only temperature measurements obtained from the intensity ratio method are independent of these stresses. Measurements using the linewidth, meanwhile, were found to correspond well with those obtained from the intensity ratio through the use of a reference condition which accounted for the stress dependency of this spectral component. These results were then compared to a three dimensional finite element model which yielded a correlation to within 5% between the computational and experimental methods. The peak position method, in contrast, was found to underpredict temperature in all circumstances due to the stress distribution which is present during device operation. © *2008 American Institute of Physics*.
[DOI: 10.1063/1.2940131]

## I. INTRODUCTION

Stemming from both a wide bandgap and large break down voltage, gallium nitride (GaN) devices are attractive for an array of applications ranging from solid-state lighting to wireless base stations and advanced military radar.[1–3] While major advancements have been achieved in the fabrication of these high performance nitride devices, widespread realization of their use has been limited, in part, due to reliability concerns.[4] These concerns are particularly relevant with respect to GaN high electron mobility transistors (HEMTs) which are capable of operating under intense electric fields and current densities thereby enabling large rf output power.[5] The same fields responsible for this high performance, however, elicit acute device heating. This heating, in turn, significantly contributes to device degradation which limits both the overall lifetime and performance of the transistor.[6–10] Thus, evaluation of this self-heating through the measurement of temperature is then critical to the realization of next generation GaN microelectronics.

While a number of techniques have been utilized in the thermometry of GaN devices, Raman spectroscopy remains one of the most widely incorporated. The 1 $\mu$m spatial resolution and relative ease of implementation have offered insight into physical phenomena previously undetectable by methods such as IR thermography.[11–18] In Raman thermometry, temperature is deduced through analysis of the inelastic energy transfer between light (photons) and lattice vibrations (phonons). As the incident light is invariant with device temperature, all deductions are then based on changes in the phonon behavior of the crystal. Thus any aspect of the phonon which changes with temperature, i.e., its population, lifetime, or energy, can then be used to probe the thermal state of the device.

Temperature measurements using Raman spectroscopy are typically carried out by analyzing changes in the energy of zone-centered optical phonons through analysis of the Stokes peak position. In such an approach, a shift in frequency of the peak is monitored and subsequently converted to temperature using an appropriate calibration standard. Often, this calibration is acquired by tracking the change in a prominent Raman peak across the temperature range of interest. Practically, this occurs by isothermally heating a sample and following the degree to which the peak shifts due to a known temperature change. Upon calibrating a GaN epilayer structure, however, there is an inherent evolution of thermoelastic stress which arises due to mismatches in the coefficients of thermal expansion between the layers. The extent to which this stress develops, in turn, affects the resulting calibration. In fact, previous research has demonstrated that differences in the Raman calibration of GaN epilayer structures may be attributed to variances in the stress states between the samples.[19] As a consequence, a calibration is strictly valid only if the stress state—at which the measurement is taken—is identical to that at which the calibration was performed.

During operation of GaN transistors, however, localized heating, as seen in Fig. 1, causes a deviation from the isothermal temperatures present during the calibration. Thus, the operational thermoelastic stress distribution will be different from that of the calibration. This difference in stress states between calibration and operation will introduce errors in the measurement of temperature using the Stokes peak

a)Electronic mail: sgraham@gatech.edu

 

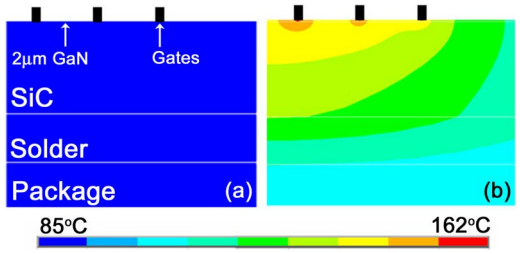


FIG. 1. (Color online) Modeled temperature contours in HEMT device during (a) calibration and (b) operation. Due to the difference in temperature distributions, the stress state during operation will be different than that of calibration. The differing stress states will contribute to errors in the measurement of temperature when utilizing the Stokes peak position.

shift. The extent of this error will be directly proportional to the degree to which these stress states deviate. Therefore, if the deviation between the stress states is minimal, then the errors will be small as well. Regardless, it is necessary to consider the stress when making Raman temperature measurements as its presence may yield large, non-negligible, errors.[19,20] Despite this fact, while some investigations have been performed with regard to both microelectromechanical systems and GaN devices, the impact of evolving stress states on Raman thermometry has received limited attention in literature.[11,19,21–23]

Stress-independent Raman measurements may be accomplished by examining the solely temperature-dependent phonon population through analysis of the ratio between the Stokes and anti-Stokes intensities.[24,25] Although theoretically simplistic, the extensive nature of this measurement makes both calibration and experimentation quite difficult in practice.[26] In addition, the integration time is at least double that of a standard Stokes analysis making the approach time intensive as well as tedious. In light of these considerations, the ideal Raman spectral component for thermal measurements would provide both the stress insensitivity of the Stokes/anti-Stokes ratio with the speed of the Stokes peak position measurement.

To this end, recent investigations have focused on performing temperature measurements utilizing the lifetime of the phonon through analysis of the linewidth of the Stokes response. This aspect of the spectrum is stress insensitive in silicon based devices thus allowing for thermal evaluation even in the presence of an evolving biaxial thermoelastic stress.[22] However, in GaN-based devices, it is unclear whether this same insensitivity will remain as stress no longer stems solely from thermally induced effects but also due to piezoelectric contributions which may affect both the energy and the lifetime of the phonon. Such ambiguity demands that the full nature of the Raman response be examined with respect to these dual stress effects in order to develop an accurate temperature measurement technique independent of their presence.

In response to these aforementioned issues, this study presents an examination of the Raman response of the $E_2^H$ phonon mode in GaN to the effects of both mechanical and inverse piezoelectric induced stress. For each of the induced stresses, the dependence of the Stokes peak position, linewidth, and Stokes/anti-Stokes intensity ratio is examined. With the knowledge of spectral dependencies, temperature measurements which account for these stress effects were then performed on two differing GaN device architectures through the use of both the Stokes linewidth and the ratio of Stokes to anti-Stokes intensities. Comparisons between measurements and a three dimensional (3D) finite element model were then made in order to validate the experimental results.

## II. DEVICE TECHNOLOGY

GaN devices utilized in this study are provided by RFMDR Inc. The devices are based on an undoped AlGaN/GaN heterostructure epitaxially grown on an optimized GaN buffer layer which itself was grown on a semi-insulating silicon carbide (SiC) substrate. A transmission line measurement (TLM) device was then created on this epilayer stack by patterning a source and drain using Ti/Al based Ohmic contacts. In the case of the TLM devices, these contacts are separated by a 20 $\mu$m channel which serves as the active region of the device. A HEMT was also fabricated on the same epilayer stack using similar source and drain contacts along with an additional 0.5 $\mu$m long Nickel Schottky barrier gate contact. Further details on the processing and composition of both the TLM and HEMT, each of which are shown schematically in Fig. 2, may be found in Refs. 27 and 28. Finally, in order to facilitate testing, the devices are wafer bonded to an alloyed copper/tungsten (Cu/W) package.

## III. RAMAN INSTRUMENTATION AND TESTING PROCEDURE

All Raman experiments were performed through the use of a Renishaw inVia Raman microscope with 180° backscattering geometry and 488 nm $Ar^+$ laser. With a spectrometer focal length of 250 mm and a diffraction grating of 3000 lines/mm, a spectral dispersion of 0.46 $cm^{-1}$/pixel was obtained at a slit width of 40 $\mu$m. A slit width of 40 $\mu$m provides an attractive balance between detection capabilities and signal levels at the expense of some spectral resolution. Even with this expense, however, the resolution is sufficient for detecting Stokes peak shifts to within $\pm 0.037$ $cm^{-1}$ from Voigt fits of the isolated $E_2^H$ GaN Raman line. A 50× objective with a numerical aperture of 0.5 was used to focus the

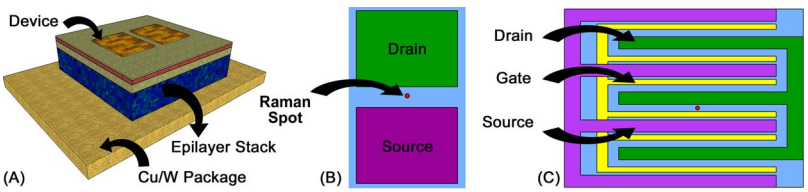


FIG. 2. (Color online) Schematic showing layout of (a) the entirety of the package, (b) TLM, and (c) HEMT including the location of the Raman spot.

probe laser beam and collect the Raman signature of the samples. Finally, to avoid laser heating of the sample, measurements were taken at decreasing levels of incident power until no change was found in the resulting spectra.

### A. Calibration of Raman spectrum with temperature

The acquisition of temperature using Raman spectroscopy necessitates an accurate calibration of the Raman response across the entirety of the temperature range of interest. To this end, the response of the GaN $E_2^H$ mode at the midpoint of a TLM device was analyzed from 23 to 500 °C in a TS-1200 Linkam heated stage. For each measurement, at least 70 separate spectra were obtained with integration times adjusted such that peak heights remained constant at ~10 000 counts. The acquired spectra were then fit using Voigt profiles in order to calculate the temperature dependency of the Stokes peak, linewidth, and ratio of Stokes to anti-Stokes intensities. After all measurements were completed, the dependencies were found to follow the expected linear, parabolic, and exponential trends for the peak position, linewidth, and intensity ratio, respectively, as is shown in Fig. 3. Through fitting of these trends, any change in the spectrum can be correlated with an equivalent change in temperature using the methods outlined in Refs. 21 and 22.

### B. Effects of mechanically induced stress on the Raman spectrum

To quantify the effect of stress on the Raman spectrum, a four-point bending test was also performed on the epilayer stack consisting of SiC, GaN, and AlGaN layers. Under increasing levels of tensile stress of up to 360 MPa applied along the basal plane (plane $\perp$ to the *c*-axis) of the GaN crystal, spectra were collected and analyzed with respect to the change in peak position, linewidth, and intensity ratio. While the induced stress was uniaxial rather than biaxial in nature, it is expected that general trends of the Raman spectrum will be similar between the different stress states as is the case in silicon.[22] The purpose of these experiments is not to determine the phonon deformation potentials for GaN, but to determine whether certain aspects of the Raman spectrum are insensitive to changes in mechanical stress.

### C. Effect of stresses arising from the inverse piezoelectric effect on the Raman spectrum

Thermoelastically induced stresses are not the sole contributor to the overall stress state during the operation of GaN transistors as the inverse piezoelectric effect is prevalent as well. Thus to understand the entirety of the stress's effect on the Raman response, a HEMT device was powered under pinch off conditions in order to induce this type of stress while simultaneously preventing device heating. The Raman response was then characterized with varying source-drain biases ranging from 10 to 48 V which in turn gave rise to varying levels of stress stemming from the inverse piezoelectric effect. With this approach, the Raman response is monitored under loads induced from the inverse piezoelectric effect independent of the Joule heating as the current is held below 0.02 mA in a manner similar to that of Sarua *et al.*[20]

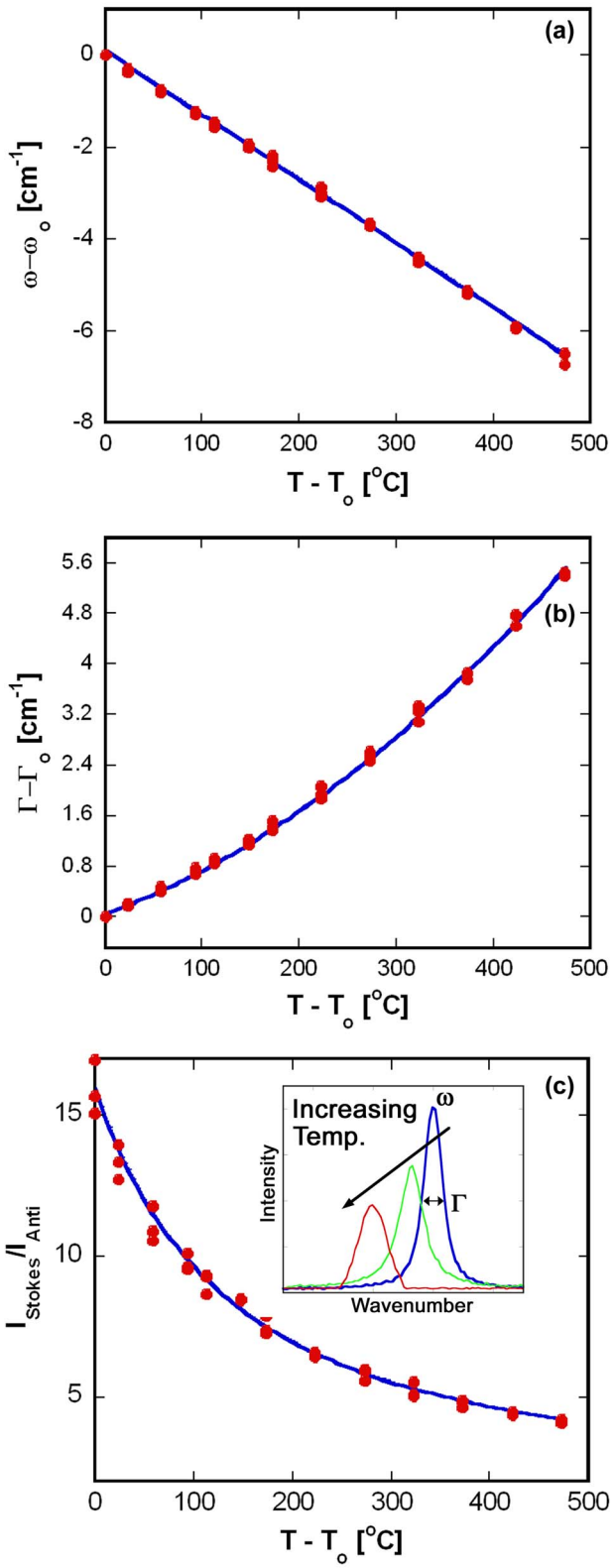


FIG. 3. (Color online) Calibration of (a) Stokes peak position, (b) Stokes linewidth, and (c) the ratio of Stokes to anti-Stokes intensity as a function of temperature at the midpoint of a packaged TLM device. The inset of (c) highlights the shifting, broadening, and reduction in intensity which occurs to the Stokes signal of the Raman response with an increase in temperature. Using these curves, any change in a spectral component may be transformed to temperature if stress induced effects are negligible.

TABLE I. Material properties utilized in model.

| Material | Property | Formula | Reference |
|---|---|---|---|
| GaN | k(T) (W/mK) | $0.0013\ T^2-1.3864\ T+547.41$ | Measured in this study |
| SiC | k(T) (W/mK) | $61100/(T-115)$ | 35 |
| Solder | k (W/mK) | 60 | Supplied by vendor |
| Cu/W package | k(T) (W/mK) | $-0.0004\ T^2-0.7492\ T+18.20$ | 36 |

### D. Device temperature measurements

Using the acquired dependencies of the Raman response to temperature and stress, temperature measurements were then carried out on both the TLM and six finger HEMT during device operation. For all measurements, samples were mounted to a controlled heated stage maintained at 85 °C using a thermal grease compound. With respect to the TLM, Raman spectra were obtained at the midpoint of the device under power dissipations of up to 6 W. At each power level, the Stokes peak shift, linewidth, and intensity ratio were used to measure temperature. A similar procedure was used in the analysis of the HEMT to examine temperatures at total dissipated power levels up to 6 W. In this case, the Raman response was acquired along the third finger at the midpoint of the channel between gate and drain halfway along the gate width, as seen in Fig. 2(c).

## IV. FINITE ELEMENT MODELING OF DEVICES

To verify the temperature measurements acquired during the Raman experiments, finite element models of both the TLM and HEMT devices were built utilizing the ANSYS software package. In order to simplify the systems under investigation, symmetry allowed for only one-quarter of the geometry to be modeled. This geometrical reduction reduced the number of elements thus speeding convergence. To capture the essential nonlinear physics of the devices, temperature dependent thermal properties were incorporated into the GaN, SiC, and Cu/W layers, as shown in Table I. With respect to the GaN, thermal conductivity values were acquired as a function of temperature through $3\omega$ testing of metal organic chemical vapor deposition–prepared GaN grown on sapphire which is of similar quality to that of the epilayer stack. Results from the test compare favorably to other reported values of thermal conductivity for GaN thin films with similar defect densities and doping profiles.[29] Further details on the $3\omega$ technique are outlined in Ref. 30.

Additional layers in the packaged devices included a solder layer between the SiC and Cu/W, as well as a simulated thermal grease layer. While the solder layer was included in the model specifically, the effects of the thermal grease layer were included through stipulation of a contact resistance between the bottom of the Cu/W package and the temperature of the heated stage (85 °C). This one dimensional (1D) approximation to the grease layer is acceptable assuming the spreading resistance is small which is likely owing to the extreme thinness of the layer.

It is important to note that the thin AlGaN layer used to generate the two dimensional (2D) electron gas at the heterointerface of the bulk GaN layer is not modeled. Typical AlGaN layers are extremely thin, typically two orders of magnitude smaller than the GaN film, thereby contributing little to the thermal signature. The nature of such a thin film also allows for the heat generation to be added into the problem as a surface heat flux boundary condition instead of an embedded volumetric heat generation. This implementation is advantageous as it significantly reduces the number of elements needed to accurately model the temperature response of the entire packaged device. All solutions then generated were checked against multiple meshes to ensure proper convergence. Convergence was defined to be the point when the maximum temperature calculated between meshes deviated by less than 1%.

Solutions generated with the finite element models allow for the temperature field to be known throughout the entirety of the 3D structure. This is not true, however, for measurements made with the micro-Raman technique. GaN is semitransparent to the 488 nm laser used in the experiments and therefore, the Raman system is essentially probing a volume of GaN instead of a distinct focal point. The resulting measurements are then a volume average through the GaN layer rather than a temperature at a distinct location. This averaging will underpredict the maximum device temperature by an amount proportional to the input power. Consequently, in order to compare the simulated results to the Raman data, the calculated temperature field was averaged through the entirety of the GaN layer using a simulated cylindrical volume 1 $\mu$m in diameter analogous to the region which is experimentally probed.

## V. THE EFFECT OF STRESS ON THE RAMAN SPECTRUM

### A. Effects of mechanically induced stress on the Raman spectrum

The effect of mechanical stresses on the Raman spectrum in GaN is shown in Fig. 4. As expected, the peak position shows a linear shift with stress. This dependency arises due to changes in the interatomic potentials occurring between each of the atoms along the direction of the load. The interatomic potential, in turn, is the greatest determinant of the phonon frequency and hence with its change comes an associated change in the peak position response.[31] As these potential changes cause the peak position to shift to higher wavenumbers with compressive loads while decreasing with higher temperature, temperature measurements during device operation are oftentimes underpredicted using this method.[21,22]

The same dependency on mechanical stress is not seen, however, in either the response of the linewidth or the ratio

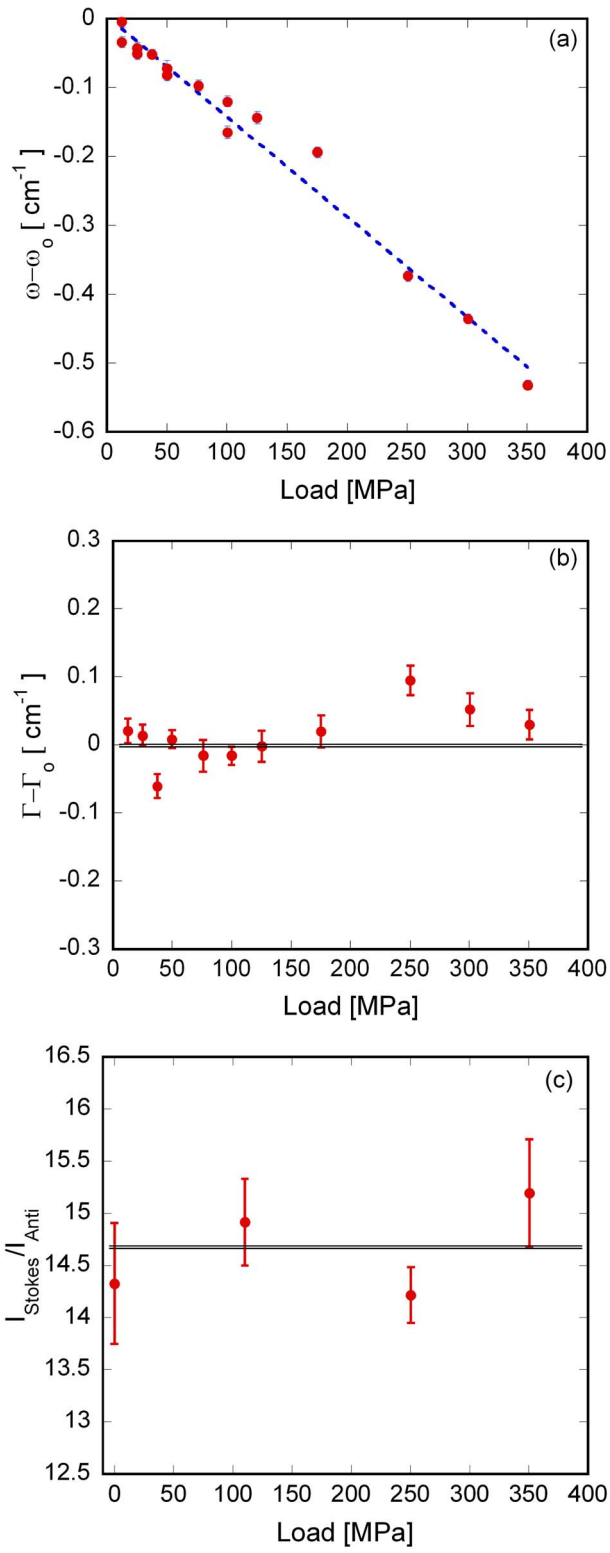


FIG. 4. (Color online) Effect of uniaxial stress on (a) Stokes peak position, (b) Stokes linewidth, and (c) Stokes/anti-Stokes ratio applied on the epilayer stack. Only the peak position shows a dependence on this mechanically induced stress along the nonpolar planar direction.

of Stokes to anti-Stokes intensities, as is shown in Fig. 4(b) and 4(c). This independence arises due to the very nature of these components' signal. For example, the Stokes/anti-Stokes intensity ratio is chiefly dependent on the population of the phonon being examined. Thus as the number of phonons is determined by the temperature dependent Bose–Einstein distribution, the resultant signal is independent of the applied stress as the phonon's population is independent to the stress' presence as well.

Similarly, the linewidth shows independence to this type of stress as its response is largely population dependent as well. Its signal arises as a consequence of the Heisenberg uncertainty relation which stipulates that a measured species, in this case the phonon, may only be measured within a certain energy band ($\Gamma$) if its availability to be measured (i.e., lifetime) is finite. This lifetime, in turn, is dependent on a variety of scattering sources including microstructural defects, material boundaries, and most importantly other phonons. As phonon-phonon scattering most often dominates, it is then both the presence of, and interaction with, other phonons which will determine the linewidth of the Raman signal. The presence of these other phonons is determined by, once again, the temperature dependent Bose–Einstein population distribution while the interaction between phonons is decided by the dispersion of the crystal lattice stemming from the interatomic potential field.[32] While the interatomic potential field certainly changes with stress, the empirical results of the bending test indicate that only a minimal change in the phonon-phonon scattering results when the stress is applied along the nonpolar basal plane of the crystal. As a result, both the linewidth and the Stokes/anti-Stokes intensity ratio may then be used to measure temperature even in the presence of a biaxial stress oriented along this basal plane as it often evolves during operation of a device.

### B. Effect of stresses arising from the inverse piezoelectric effect on the Raman spectrum

Unlike the 1D electric field present during operation of a TLM structure, a 2D field forms upon activation of the HEMT device. The 2D field will be oriented in such a way that a planar component will be directed along the vector pointing from the source to the drain while a separate through thickness (vertical) contribution will form along the polar [0001] direction of the GaN crystal due the presence of the gate.[20] These electric fields will subsequently induce strains in the material due to the inverse piezoelectric effect. Since GaN has only three independent nonzero components of the piezoelectric modulus, a shear strain is the sole component present during the operation of the TLM.[33,34] During operation of a HEMT, meanwhile, this same shear strain is augmented by axial strains along each the three principal directions resulting from the vertical field component. The final stress state of the device will then result from these induced strains and the subsequent constraint to deformation supplied by the underlying SiC and any gradients which are present in the electric field. Disparate from the four-point bending test, it is of particular importance that the resulting stress state will have a nonzero component along the polar ($\parallel$ to the $c$-axis) [0001] direction.

To examine if the induced stress along the polar direction affects the Raman response, a HEMT device was examined under pinch off conditions allowing for the development

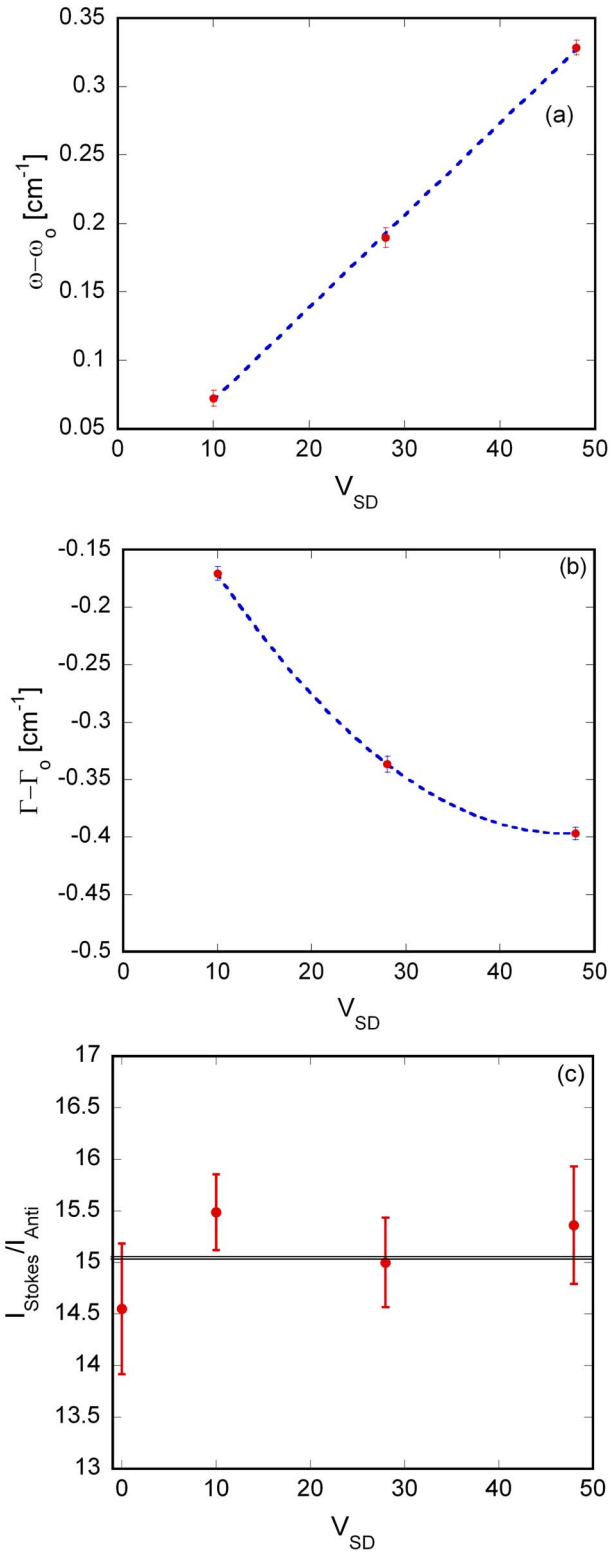


FIG. 5. (Color online) Effect of stress arising from the inverse piezoelectric effect on (a) the Stokes peak position, (b) linewidth, and (c) the Stokes to anti-Stokes intensity ratio applied through biasing of a HEMT under pinch off conditions. Unlike that seen for loading along the nonpolar direction, the induced stress along the polar (vertical) direction of the crystal affects the linewidth signal.

of inverse piezoelectric induced stresses apart from joule heating. Shown in Fig. 5 is the effect of this loading on the Raman response for each of the examined aspects of the spectrum. Similar to that which was seen in the mechanically induced stress, the peak position displays a linear dependence with increasing source-drain voltage indicating that the final stress is indeed directly proportional to the applied field. The linewidth, meanwhile, is dependent on the level of this stress arising from the inverse piezoelectric effect as well. This result is contrary to the initial four-point bending investigation and indicates that unlike the planar load, a polar stress distorts the dispersion to an extent which affects scattering and hence the linewidth. Thus when subject to stresses arising from the inverse piezoelectric effect, such as those present during HEMT operation, the linewidth, unless in some way corrected, will induce errors in the measurement of temperature. Without a correction to the linewidth, it is then necessary to utilize the Stokes to anti-Stokes intensity ratio to measure temperature as this metric is insensitive to both types of loading, as is shown in Figs. 4(c) and 5(c).

## VI. MEASUREMENT OF DEVICE TEMPERATURE

### A. TLM device

To investigate the capability of Raman thermometry in the presence of an evolving thermoelastic stress, a TLM device was probed at a package temperature of 85 °C under dissipative powers of up to 6 W. In order to completely assess the capability of measuring temperature at these large loads, each aspect of the Raman spectrum was utilized. Regardless of the method, temperature was obtained by comparing the difference in the Raman spectra between the unpowered reference ($V_{SD}$=0) and powered states. The spectral difference was then transformed to a temperature using the appropriate calibrations shown in Fig. 3 and subsequently compared to the finite element model in order to assess the suitability of each method. At least 50 separate spectra were acquired at each experimental condition such that the resulting uncertainties in the temperature measurement were +/−0.4, 1.4, and 3.8 °C for the peak position, linewidth, and Stokes/anti-Stokes intensity ratio, respectively.

The resulting trends of temperature versus power are shown in Fig. 6 for each of three aspects of the Raman spectra as well as the computational model. Values of the measured temperature derived from both the linewidth and Stokes to anti-Stokes ratio correlate well with those of the model indicating the accuracy of each technique. Meanwhile, the evolution of the thermoelastic stress causes the peak position to underpredict the temperature by as much as 50 °C in a manner similar to that which occurs during the operation of silicon devices.[21,22] These results indicate the efficacy of using either the linewidth or intensity ratio even in the presence of thermal stresses without the need for any correction procedures.

Derived from these measurements, a separate conclusion can be made with regard to the sensitivity of the linewidth to stresses arising from the inverse piezoelectric effect. As shown in the previous section, the linewidth is modified with the application of the 2D electric field present during operation of a HEMT. In a TLM, this field is 1D in nature and acts to produce only a shear stress in the material. As the TLM cannot be operated under "pinch off" conditions like the HEMT, it is unclear whether this shear stress will affect the

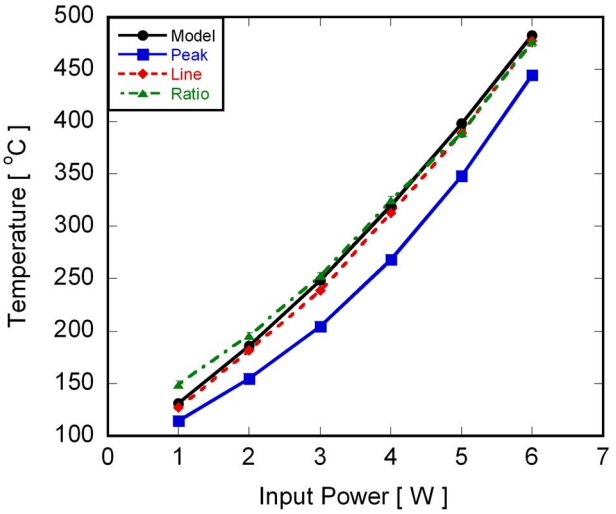


FIG. 6. (Color online) Operating temperature of TLM device as a function of dissipated power at a package temperature of 85 °C. The temperature measured using both the linewidth and Stokes/anti-Stokes ratio correlating well with the prediction of the computational model. The peak position significantly underpredicts the temperature as it is affected by the presence of the evolving thermoelastic stress.

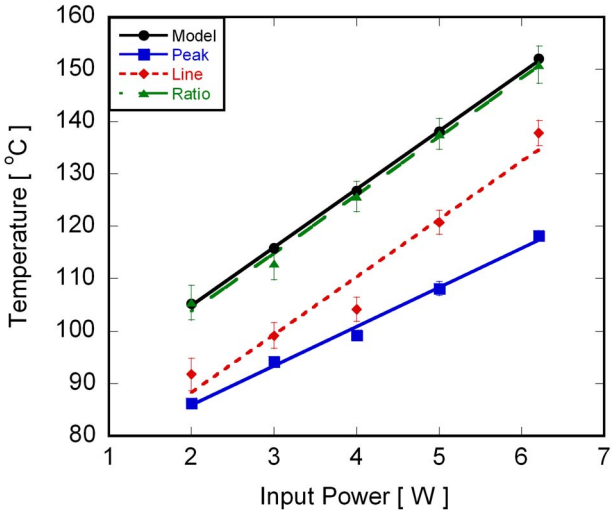


FIG. 7. (Color online) Operating temperature of a HEMT at a package temperature of 85 °C acquired from Raman measurements derived using a standard unpowered reference condition. Only the measurements obtained from the Stokes to anti-Stokes intensity ratio correlate with the predicted operating temperatures due to this aspect's independence to both thermally and piezoelectric induced stresses.

linewidth. The subsequent temperature measurements using the linewidth, however, show distinct correlation with estimates of both the Stokes/anti-Stokes ratio as well as the model, thereby indicating that this shear stress induced from the inverse piezoelectric effect must minimally affect the linewidth. Therefore, it is the vertical field acting along the polar direction of the crystal present only during HEMT operation which is the dominant piezoelectric component and causes the subsequent changes in the linewidth.

### B. HEMT device

Following a procedure similar to that undertaken in the analysis of the TLM device, the HEMT was investigated at a package temperature of 85 °C under increasing levels of power dissipation up to 6 W (2.5 W/mm) with a source-drain bias ($V_{SD}$) of 28 V. Once again, each aspect of the Raman spectrum was used to evaluate temperature whereupon the efficacy of each method was evaluated through comparison with the multiphysical computational model. In this case, at least 70 separate spectra were acquired at each experimental condition such that the resulting uncertainties in the temperature measurement were +/−0.89, 2.5, and 3.1 °C for the peak position, linewidth, and Stokes/anti-Stokes intensity ratio, respectively. Shown in Fig. 7 are the derived trends for temperature versus power for each of the different techniques. Due to its sole temperature dependence, measurements derived from the Stokes to anti-Stokes intensity ratio are found to be closely correlated with the estimations of the model. The result indicates the ability of the intensity ratio to measure temperature independent of the stress state in GaN devices. Both the linewidth and the peak position, however, significantly underpredict the temperature due to the influence of the complex stress state arising from the dual effects of both the piezoelectric and thermally induced stresses. Consequently, in order to obtain a quick and accurate Raman thermometry method, the effects of these complex stresses must in some way be removed.

Sarua *et al.* asserted that the level of piezoelectric induced stress will be similar regardless of whether the gate on the transistor channel is opened or closed.[20] By following these results, errors in the temperature measurement arising due to the inverse piezoelectric effect may then be removed by simply comparing the difference in the Raman spectra between the powered and pinch off, rather than unpowered, reference states. Practically this is implemented by acquiring the reference state $(\omega_0,\Gamma_o)$ under the pinch off conditions ($V_{SD}$=28 V, $V_G$=−8 V) rather than the completely unpowered state ($V_{SD}$=0 V, $V_G$=0 V) and once again measuring the operating temperature of the HEMT. As shown in Fig. 8, it is clear that indeed the piezoelectric contribution may be removed using the pinch off reference condition as the measurements of temperature derived from the linewidth now show clear correlation to both the estimates from the intensity ratio as well as the model. However, despite the removal of the piezoelectric contribution, the peak position continues to underpredict temperature as thermoelastic stresses remain a significant source of error. Nonetheless, through utilization of the pinch off reference condition, the linewidth allows for a Stokes Raman temperature measurement independent of the complex stress states which arise during GaN transistor operation.

## VII. CONCLUSION

Operating temperature is a key determinant in both the reliability and performance of GaN devices thus making the parameter's measurement central to further development. Raman thermometry is an attractive tool for the acquisition of these temperatures as it is noninvasive and has a spatial and temporal resolution on par with that of the device. How-

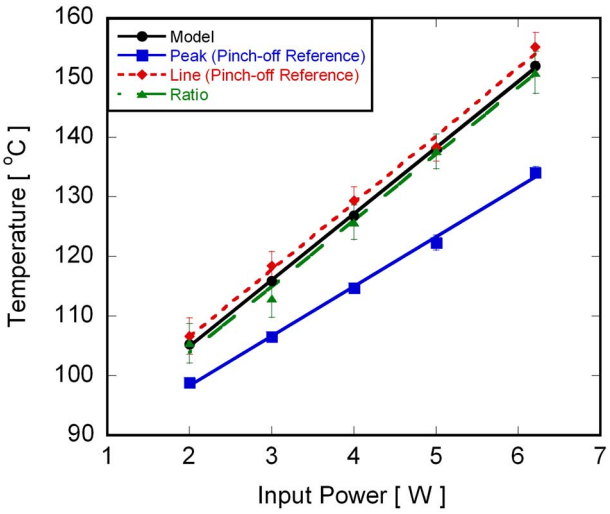


FIG. 8. (Color online) Operating temperature of a HEMT measured using Raman spectroscopy with a reference taken under pinch off conditions. Using this nonstandard reference condition allows for piezoelectric induced effects to be removed thus allowing for the accurate measurement of temperature through use of the Stokes linewidth.

ever, the technique's accuracy is limited by errors induced by stresses arising from both thermoelastic and piezoelectric contributions. This study has examined the manner in which these stresses affect the three different aspects of the Raman spectrum which may be used to measure temperature, namely, the Stokes peak position, linewidth, and the Stokes to anti-Stokes intensity ratio. In the course of examining their dependencies, it was found that only the intensity ratio was independent to all stress components while the linewidth was sensitive to the stresses induced along the polar direction of the crystal owing to the inverse piezoelectric effect. Thus only the intensity ratio was capable of accurately measuring temperature independent of all stress contributions. However, during the measurement of a transistor device, piezoelectric induced errors in the linewidth measurements were removed through the utilization of a pinch off reference condition allowing for utilization of only the Stokes response in thermal estimation. As peak position remains subjected to thermal stresses even after piezoelectric contributions are removed, future studies may quantify the level of stress in a device by monitoring the differences in the reported temperatures between this method and either the linewidth or intensity ratio.

## ACKNOWLEDGMENTS

This work was supported in part by the NSF CAREER Grant No. CTS-0448795 and the Air Force Research Laboratory (AFRL) Materials & Manufacturing Directorate.

[1]K. Gurnett and T. Adams, III-Vs Review **19**, 20 (2006).
[2]L. Kim, G. W. Lee, W. J. Hwang, J. S. Yang, and M. W. Shin, Phys. Status Solidi C **0**, 2261 (2003).
[3]J. Shealy, J. Smart, M. Poulton, R. Sadler, D. Grider, S. Gibb, B. Hosse, B. Sousa, D. Halchin, V. Steel, P. Garber, P. Wilkerson, B. Zaroff, J. Dick, T. Mercier, J. Bonaker, M. Hamilton, C. Greer, and M. Isenhour, Gallium Arsenide Integrated Circuit (GaAs IC) Symposium, 24th Annual Technical Digest, 2002 (unpublished).
[4]M. Kuball, M. J. Uren, and T. Martin, Semiconductor Device Research Symposium, 2005 (unpublished).
[5]J. Joh and J. A. del Alamo, Electron Devices Meeting, IEDM '06. International, 2006 (unpublished).
[6]I. Daumiller, C. Kirchner, M. Kamp, K. J. Ebeling, and E. Kohn, IEEE Electron Device Lett. **20**, 448 (1999).
[7]H. Kim, V. Tilak, B. M. Green, J. A. Smart, W. J. Schaff, J. R. Shealy, and L. F. Eastman, Phys. Status Solidi A **188**, 203 (2001).
[8]S. Singhal, T. Li, A. Chaudhari, A. W. Hanson, R. Therrien, J. W. Johnson, W. Nagy, J. Marquart, P. Rajagopal, J. C. Roberts, E. L. Piner, I. C. Kizilyalli, and K. J. Linthicum, Microelectron. Reliab. **46**, 1247 (2006).
[9]R. Vetury, J. B. Shealy, D. S. Green, J. McKenna, J. D. Brown, S. R. Gibb, K. Leverich, P. M. Garber, and M. J. Poulton, IEEE MTT-S International Microwave Symposium Digest 2006 (unpublished).
[10]Y. Zhu and H. D. Espinosa, Int. J. RF Microwave Comput.-Aided Eng. **14**, 317 (2004).
[11]J. Kim, J. A. Freitas, J. Mittereder, R. Fitch, B. S. Kang, S. J. Pearton, and F. Ren, Solid-State Electron. **50**, 408 (2006).
[12]J. Pomeroy, M. Kuball, D. Wallis, A. Keir, P. Hilton, R. Balmer, M. Uren, and T. Martin, Appl. Phys. Lett. **87**, 103508 (2005).
[13]M. Kuball, J. M. Hayes, M. J. Uren, T. Martin, J. C. H. Birbeck, R. S. Balmer, and B. T. Hughes, IEEE Electron Device Lett. **23**, 7 (2002).
[14]Y. Ohno, M. Akito, S. Kishimotoa, K. Maezawa, and T. Mizutani, Phys. Status Solidi C **0**, 57 (2002).
[15]R. Aubry, C. Dua, J. C. Jacquet, F. Lemaire, P. Galtier, B. Dessertenne, Y. Cordier, M. A. DiForte-Poisson, and S. L. Delage, Eur. Phys. J.: Appl. Phys. **30**, 77 (2005).
[16]I. Ahmad, V. Kasisomayajula, D. Y. Song, L. Tian, J. M. Berg, and M. Holtz, J. Appl. Phys. **100**, 113718 (2006).
[17]I. Ahmad, V. Kasisomayajula, M. Holtz, J. M. Berg, S. R. Kurtz, C. P. Tigges, A. A. Allerman, and A. G. Baca, Appl. Phys. Lett. **86**, 173503 (2005).
[18]Y. Ohno, M. Akita, S. Kishimoto, K. Maezawa, and T. Mizutani, Jpn. J. Appl. Phys., Part 2 **41**, L452 (2002).
[19]J. Kim, J. A. Freitas, Jr., P. B. Klein, S. Jang, F. Ren, and S. J. Pearton, Electrochem. Solid-State Lett. **8**, G345 (2005).
[20]A. Sarua, J. Hangfeng, M. Kuball, M. J. Uren, T. Martin, K. J. Nash, K. P. Hilton, and R. S. Balmer, Appl. Phys. Lett. **88**, 103502 (2006).
[21]M. R. Abel, S. Graham, J. R. Serrano, S. P. Kearney, and L. M. Phinney, J. Heat Transfer **129**, 329 (2007).
[22]T. Beechem, S. Graham, S. Kearney, L. Phinney, and J. Serrano, Rev. Sci. Instrum. **78**, 061301 (2007).
[23]A. Sarua, M. Kuball, and J. E. V. Nostrand, Appl. Phys. Lett. **85**, 2217 (2004).
[24]G. Burns, F. Dacol, J. C. Marinace, B. A. Scott, and E. Burstein, Appl. Phys. Lett. **22**, 356 (1973).
[25]G. Abstreiter, Appl. Surf. Sci. **50**, 73 (1991).
[26]F. LaPlant, G. Laurence, and D. Ben-Amotz, Appl. Spectrosc. **50**, 1034 (1996).
[27]J. D. Brown, S. Gibb, J. McKenna, M. Poulton, S. Lee, K. Gratzer, B. Hosse, T. Mercier, Y. Yang, M. Young, D. Green, R. Vetury, and J. Shealy, ECS Trans. **3**, 161 (2006).
[28]J. D. Brown, S. Lee, D. Lieu, J. Martin, R. Vetury, M. J. Poulton, and J. B. Shealy, IEEE/MTT-S International Microwave Symposium, 2007 (unpublished).
[29]A. Jezowski, B. A. Danilchenko, M. Bockowski, I. Grzegory, S. Krukowski, T. Suski, and T. Paszkiewicz, Solid State Commun. **128**, 69 (2003).
[30]B. W. Olson, S. Graham, and K. Chen, Rev. Sci. Instrum. **76**, 053901 (2005).
[31]G. Lucazeau, J. Raman Spectrosc. **34**, 478 (2003).
[32]D. Y. Song, S. A. Nikishin, M. Holtz, V. Soukhoveev, A. Usikov, and V. Dmitriev, J. Appl. Phys. **101**, 053535 (2007).
[33]F. Bernardini and V. Fiorentini, Appl. Phys. Lett. **80**, 4145 (2002).
[34]J. F. Nye, *Physical Properties of Crystals: Their Represenation by Tensors and Matrices* (Clarendon, Oxford, 1979).
[35]O. Nilsson, H. Mehling, R. Horn, J. Fricke, and R. Hofmann, High Temp. - High Press. **29**, 73 (1997).
[36]Y. D. Kim, N. L. Oh, S. T. Oh, and I. H. Moon, Mater. Lett. **51**, 420 (2001).